Fabrication of a Photoelectronic Device by Direct Chemical Binding of the Photosynthetic Reaction Center Protein to Metal Surfaces

4 AUTHORS, INCLUDING:

Yossi Rosenwaks
Tel Aviv University
181 PUBLICATIONS **3,094** CITATIONS

SEE PROFILE

Itai Carmeli
Tel Aviv University
37 PUBLICATIONS **737** CITATIONS

SEE PROFILE

COMMUNICATIONS

[13] M. Shim, A. Javey, N. W. S. Kam, H. J. Dai, *J. Am. Chem. Soc.* **2001**, *123*, 11 512.

[14] T. Takenobu, T. Takano, M. Shiraishi, Y. Murakami, M. Ata, H. Kataura, Y. Achiba, Y. Iwasa, *Nat. Mater.* **2003**, *2*, 683.

[15] S. M. Sze, *Physics of Semiconductor Devices*, Wiley, New York **1981**.

[16] C. Klinke, J. Chen, A. Afzali, Ph. Avouris, *Nano Lett.* **2005**, *3*, 555.

[17] S. Auvray, V. Derycke, M. Goffman, A. Filoramo, O. Jost, J. P. Bourgoin, *Nano Lett.* **2005**, *3*, 451.

[18] S. Kazaoui, Y. Guo, W. Zhu, Y. Kim, N. Minami, *Synth. Met.* **2003**, *135*, 753.

[19] J. Lu, S. Nagase, D. P. Yu, H. Q. Ye, R. S. Han, Z. X. Gao, S. Zhang, L. M. Peng, *Phys. Rev. Lett.* **2004**, *93*, 116 804.

[20] H. Kataura, Y. Maniwa, M. Abe, A. Fujiwara, T. Kodama, K. Kikuchi, H. Imahori, Y. Misaki, S. Suzuki, Y. Achiba, *Appl. Phys. A* **2002**, *74*, 349.

[21] M. Shiraishi, T. Takenobu, A. Yamada, M. Ata, H. Kataura, *Chem. Phys. Lett.* **2002**, *358*, 213.

[22] K. Bradley, J.-C. P. Gabriel, M. Briman, A. Star, G. Grüner, *Phys. Rev. Lett.* **2003**, *91*, 218 301.

[23] T. Kanbara, T. Iwasa, K. Tsukagoshi, Y. Aoyagi, Y. Iwasa, *Appl. Phys. Lett.* **2004**, *85*, 6404.

[24] A. Javey, J. Guo, B. F. Damon, Q. Wang, D. Wang, R. G. Gordon, M. Lundstrom, H. J. Dai, *Nano Lett.* **2004**, *4*, 447.

[25] F. Léonard, J. Tersoff, *Phys. Rev. Lett.* **2000**, *84*, 4693.

[26] A. Zangwill, *Physics at Surfaces*, Cambridge University Press, Cambridge, UK **1988**.

[27] S. Kobayashi, T. Nishikawa, T. Takenobu, S. Mori, T. Shimoda, T. Mitani, H. Shimotani, N. Yoshimoto, S. Ogawa, Y. Iwasa, *Nat. Mater.* **2004**, *3*, 317.

Fabrication of a Photoelectronic Device by Direct Chemical Binding of the Photosynthetic Reaction Center Protein to Metal Surfaces**

By *Ludmila Frolov, Yossi Rosenwaks, Chanoch Carmeli,* and *Itai Carmeli*

Photosystem I (PS I) is a transmembrane, multi-subunit protein–chlorophyll complex that mediates vectorial, light-induced electron transfer. The nanometer-sized dimensions, an energy yield of approximately 58 %, and the quantum effi-

[*] Prof. C. Carmeli, L. Frolov
Department of Biochemistry, Tel Aviv University
Tel Aviv 69978 (Israel)
E-mail: ccarmeli@post.tau.ac.il
Prof. Y. Rosenwaks
Department of Physical Electronics, Tel Aviv University
Tel Aviv 69978 (Israel)
Dr. I. Carmeli
Department of Physics, University of California
Santa Barbara, CA 93106 (USA)

ciency of almost 1[1] make the reaction center a promising unit for applications in molecular nanoelectronics. PS I is located in the thylakoid membranes of chloroplasts and cyanobacteria. It mediates light-induced electron transfer from plastocyanin or cytochrome C_{553} to ferredoxin.[2,3] The crystalline structure of PS I from *Synechococus elongatus* and from plants' chloroplast was resolved to 2.5 and 4.4 Å, respectively.[4,5] In cyanobacteria, the complex consists of at least 12 polypeptides, some of which bind 96 light-harvesting chlorophyll molecules. The electron-transport chain contains P700, A_0, A_1, F_X, F_A, and F_B, representing a chlorophyll *a* dimer, a monomeric chlorophyll *a*, two phylloquinones, and three [4Fe–4S] iron–sulfur centers, respectively. The reaction-center core complex is made up of the heterodimeric PsaA and PsaB subunits, containing the primary electron donor, P700, which undergoes light-induced charge separation and transfers an electron through the sequential carriers A_0, A_1, and F_X. The final acceptors, F_A and F_B, are located on another subunit, PsaC. The redox potential of the primary donor, P700, is +0.43 V and that of the final acceptor, F_B, is –0.53 V, producing a redox difference of –1.0 V. The charge separation spans about 5 nm of the height of the protein, representing the center-to-center distance between the primary donor and the final acceptor. The protein complex is 9 nm in height and has a diameter of 21 nm and 15 nm for the trimer and the monomer, respectively.[4] The photoactivity and the nanometer-sized dimensions make this complex a promising unit for applications in molecular nanoelectronics. In earlier works, care was taken to indirectly attach plant PS I[6,7] and bacterial reaction centers[8,9] to solid surfaces in attempts avoid inactivation of self-assembled monolayers.

In this work, we devised a system that overcame the problems arising from direct covalent binding of proteins to metal surfaces. We selected the robust PS I reaction centers from the cyanobacteria *Synechocystis sp.* PCC 6803. The main reason for the structural stability of this PS I is due to the fact that all chlorophyll molecules and carotenoids are integrated into the complex of core subunits, while, in plant and bacterial reaction centers, the antenna chlorophylls are bound to chlorophyll–protein complexes that are attached to the core subunits. Indeed, there was no need to use peptide surfactants, which were essential for stabilization of plant PS I and the bacterial reaction centers.[7] A careful selection of the amino acids, which were modified to cysteines for covalent attachment of the PS I to the gold surface, was the second factor that insured structural and functional stability of the self-assembled, oriented PS I. The rational design was based on the knowledge of the atomic structure of PS I. Amino acids, which do not have stereo hindrance when placed on a solid surface, were mutated to cysteines in order to insure formation of sulfide bonds (Figs. 1a,b) in the extra membrane loops facing the cytoplasmic side of the bacterial membrane. The various mutations were selected near the P700 to ensure close proximity between the reaction center and the gold electrode in order to facilitate an efficient electric junction. Cysteines D479C, S499C, S599C, and Y634C were placed at an increas-

DOI: 10.1002/adma.200500295

ing distance from the P700 to be able to mini-mize the disturbance in the function of the reaction center with the efficiency of the electronic junction. Although the protein contains nine free cysteines, none of them was found to be exposed to an external surface when tested with the surface-active reagent, biotin-maleimide. Yet PS I complexes from mutants D479C, S499C, S599C, and Y634C were modified by biotin-maleimide. Therefore, the cysteinyl residues introduced into these strains were exposed on the surface, as expected from amino acid residues that are located at the extra-membrane loops in PS I. The mutations did not modify the photochemical properties and the subunit composition of the isolated PS I, as shown below.

The fabrication of oriented monolayers was carried out by directly reacting the cysteine in the mutant PS I with a fresh, clean, hydrophilic gold surface to form an Au–sulfide bond. A flat gold surface was prepared by evaporation of 5 nm of Cr and 150 nm of gold on glass or silicon wafers. These surfaces were annealed at 350 °C for 1 h under vacuum. PS I mutants self-assembled on the gold surfaces. Following incubation for 2 h at room temperature to form sulfide bonds, the unattached proteins were thoroughly washed several times with distilled water in a fashion that left only the covalently bound PS I attached to the gold surface. The surface was dried with ultrapure nitrogen. Indeed, native PS I complexes, which were incubated in a similar manner, were washed away from the gold surface. Atomic force microscopy (AFM) images obtained by a scan of a 0.3 μm × 0.3 μm area of the gold surface on the glass slide, to which trimers of PS I cysteine mutant D479C were attached through sulfide bonds, clearly shows a monolayer of particles 15–21 nm in diameter and 9 nm high (Fig. 2a). This is the expected size of PS I as obtained by crystallography. These particles are seen over the lightly granulated surface. The annealed, untreated, bare gold surface con-
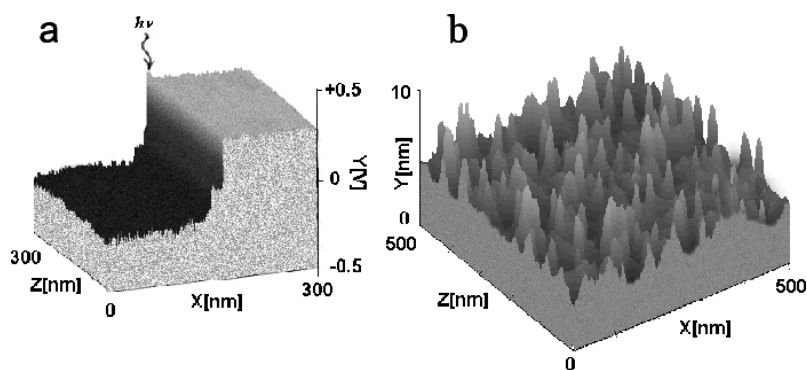

Figure 2. Three-dimensional (3D) topographic and electric potential images of oriented PS I reaction centers on the gold surface. a) An electric potential image of a PS I reaction center monomers on an Au–Si surface was measured. A light-induced PS I positive electrical potential of PS I is seen on illuminating it by a He–Ne laser at 632.8 nm, 5 mW cm^{-2} (hν). b) 3D topographic presentation of PS I trimer on Au–Si substrate. The scanning directions for each raster of the constructed images were from top to bottom (from dark to light). The negative sign of the potential shown in the (a) is due to the Kelvin probe force microscope feedback circuit and is opposite to the actual sign of the CPD.

tain gold granules 150 nm in diameter and 5 nm high, which are much larger than the PS I (see Supporting Information).

Photovoltage measurements were taken by Kelvin probe force microscopy (KPFM) of PS I complexes of cysteine mutant D479C in the monolayer. The KPFM image demonstrates a clear, light-induced, positive electric potential in PS I monomers (Fig. 2b). The light-induced positive potential of +0.498 ± 0.02 V was developed (Table 1, Figs. 3b,d) where peaks ascribed to single PS I trimer complexes were observed

Table 1. Light-induced electric potential of PS I monolayers. Electric potential of PS I reaction center monomers and trimers from the mutant D479C monolayer on a Au–Si surface. Each value is an average of 24 individual PS I measured in the dark or in the light. Illumination was provided by a He–Ne laser at 632.8 nm, 5 mW cm^{-2}.

PS I/ Potential	Dark [V]	Light [V]	Light–Dark [V]	
			From light to dark	From dark to light
Monomer	−0.193 ± 0.0005	+0.118 ± 0.0010	+0.311 ± 0.0010	–
Monomer	−0.353 ± 0.0002	+0.004 ± 0.0006	–	+0.356 ± 0.001
Trimer	+0.870 ± 0.003	+1.220 ± 0.0200	+0.358 ± 0.0014	–
Trimer	+0.717 ± 0.003	+1.215 ± 0.0200	–	+0.498 ± 0.020

in the topographic trace (Figs. 3a,c). These results clearly indicate that all PS I complexes bound to the gold surface were functionally active and oriented in the same direction. PS I orientation was also shown by the changes observed in the X-ray fluorescence of the iron K edge as a function of the change in the angle relative to the polarized X-ray beam, as determined by total-reflection measurements of grazing X-ray fluorescence (not shown). The induced potential is a result of a negative-charge displacement away from the gold side of PS I, as shown in Figure 1b. The measured change in contact potential difference (CPD) under illumination is in good
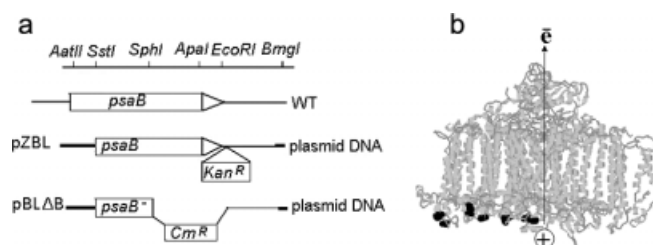

Figure 1. The cysteine mutations. a) Scheme of the vectors used for induction of mutations in psaB of *Synechocystis sp.* PCC 6803 by homologous recombination. Plasmids pZBL and pBLΔB were constructed for insertion of mutations and selection of psaB-deficient recipient cells, respectively. b) Backbone presentation of the structure of PS I with the proposed mutations D235C, S246C, D479C, S499C, S599C, and Y634C in the PsaB subunit in "spacefill" (Protein Data Bank, PDB, file JBO1). The arrow shows the direction of light-induced charge transfer.
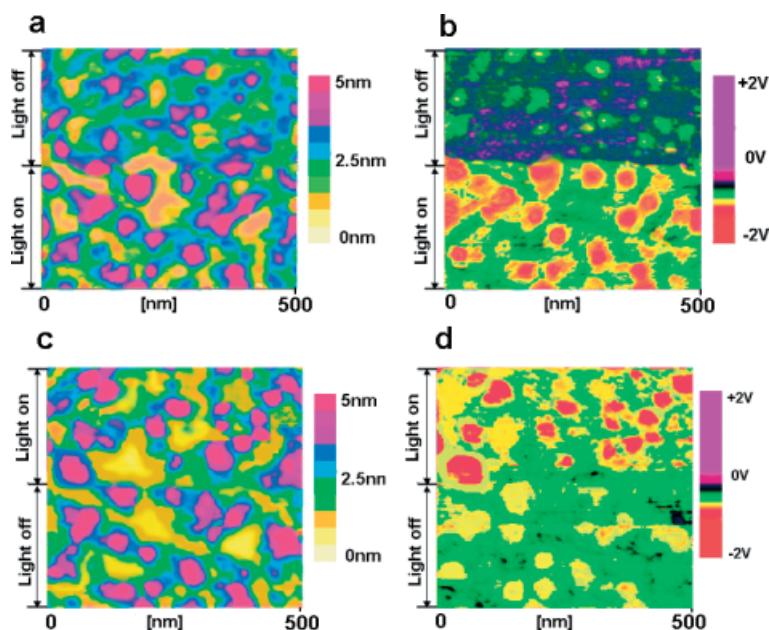
Figure 3. Two-dimensional spatial and electric potential maps of oriented PS I reaction centers on gold surface. a,c) Topographic and b,d) electric potential images of the same set of PS I reaction center trimers from mutant D479C on a Au–Si surface. A light-induced negative electrical potential of PS I is seen in (b,d). The illumination, provided by a He–Ne laser at 632.8 nm, 5 mW cm^{-2}, was turned on and off where indicated on the image.

work function also increased by approximately +0.125 V during illumination. Partial charge transfer to the vicinity of the photo-oxidized P700, which is located at the interface of PS I and the metal, is expected to result in a more negative substrate. The charge transfer is indicative of efficient electronic coupling between the gold and PS I. There was, however, very little change in the CPD when the untreated gold surface was illuminated. It can also be seen that the PS I complexes had a slightly more positive potential (CPD of +0.2 V) than the gold substrate in the dark (Fig. 3b). This potential might have resulted from excitation of PS I by the AFM feedback laser, which was not completely masked by the cantilever used in the KPFM setup. Such background excitation might cause an underestimation of the light-minus-dark CPD (SPV) change in PS I. A similar potential was attributed to permanent charge resulting from local surface concentration of negatively charged amino acids at the ferredoxin docking site at the electron donor end of PS I.[6]

The reversible nature of the light-induced electric potential was demonstrated in an experiment in which a change in the potential was observed when the illumination was turned off. The illuminated trimers of PS I cysteine mutants in the monolayer developed a CPD of +1.220 ± 0.02 V that decreased to +0.870 ± 0.003 V when the light was turned off (Table 1 and Fig. 3d). These values represent an average potential of multiple PS I complexes measured either in the light or in the dark, as shown in Table 1. The substrate potential did not change when the light was turned off. Under the applied bias potential in the experiments, charges could not move quickly to the bulk gold substrate from the vicinity of PS I. Therefore, the SPV was smaller when the light was turned off compared to the difference when turning the light on (Table 1). The average SPV of multiple PS I complexes was +0.358 ± 0.014 V. There was no change in the contact potential where the gold surface was exposed. The photopotential could be reproduced multiple times and repeatedly on the same sample or on a sample that was stored for over a month.

The PS I monomer of the cysteine mutant D479C readily formed self-assembled, oriented monolayers. The average distance between the monomers and the trimers in the monolayers was 15 nm and 25 nm, respectively. The small monomers were more densely packed than the trimers in the monolayer, yet the monomers could be resolved by the AFM measurements with the high-resolution cantilever tip (see Supporting Information). However, neither the topography nor the CPD measurements were sensitive enough to resolve the individual monomers. Therefore, the CPD of the PS I monomer monolayer obtained by KPFM measurements in the dark describes a continuum (Fig. 1a). A similar image was observed when the topography was determined by the same

agreement with a simple calculation of the potential change ($\Delta\Phi$) resulting from an induced dipole layer of height d, at an angle $\check{\iota}$ with respect to the surface normal, given by:

$$\Delta\Phi = Nqd(\cos\check{\iota})/\varepsilon \qquad (1)$$

where N is the area density of the dipole layer, q is the elementary charge, and ε is the layer dielectric constant. Using a value for N of 2.2×10^{11} cm^{-2} for the trimer, $d = 5$ nm, $\varepsilon = 2$, and $\check{\iota} = 90°$, we obtain $\Delta\Phi = 0.41$ V. The discrepancy between the expected +1 V and the calculated 0.41 V is partially resolved because the angle of the dipoles in the layer is not known, and also the dielectric constant is an ill-defined property since the dipole layer is not a bulk entity. Moreover, as the reaction centers were relatively far from each other, the measured CPD under illumination was much less then the real CPD. Due to the long-range electrostatic forces, the measured CPD at a point on the surface below the tip apex is a weighted average of the surface potential in the vicinity of the tip. The effect of the tip electrostatic average was calculated in the past using different algorithms.[10] Based on these calculations, it is estimated that the real CPD (under illumination) is around a factor of two larger than the measured one. Similar light-induced potential was measured in plant PS I placed on mercaptoethanol-coated gold. The PS I was insulated from the gold by mercaptoethanol and formed only a loosely bound monolayer, in which only 70 % of the complexes assumed the same orientation.[6] It should be noted that the gold-surface

setup (not shown). Yet, on turning the light on, the CPD increased. An average of measurements of CPD at multiple locations on the monolayer in the dark and in the light gave a light-induced CPD of +0.356 ± 0.001 V (Table 1). A smaller, light-induced CPD of +0.311 ± 0.001 V was observed when the change was determined on turning off the illuminated monolayer.

Self-assembly of oriented PS I was also obtained with the three other mutants, in which the amino acids S499C, S599C, and Y634C, located at the exposed extra-membrane loops, were modified to cysteines (Fig. 1b). Both monomers and trimers of PS I of these mutants formed monolayers that generated light-induced CPD of similar magnitude to the one measured in monolayers made of mutant D479C. It therefore seems that a functionally oriented monolayer of PS I depends on the formation of a sulfide bond between a cysteine and the gold surface located at the extra-membrane loop of the complex and is not confounded to a specific location.

To characterize the effects of the mutations on the electron transfer in the PS I complexes, flash-induced absorption changes were measured by single turnover spectroscopy as earlier described.[11] The flash-induced transient decay, ΔA, at 820 and 700 nm in PS I proteins isolated from mutants D479C, showed a similar result as for the wild type, with a back reaction of 4.5 ms halftime, which should be ascribed to the reduction of P700$^+$ by the electron-transfer mediator, phenasine methosulfate (see Supporting Information). The results indicated that electrons are mediated to F_A/F_B in the mutated PS I.

It was demonstrated for the first time in this work that selection of a robust reaction center PS I from cyanobacteria and rational design of mutations based on the crystallographic structure enable the fabrication of an oriented monolayer on a conducting metal surface. Direct binding of the protein complex to the metal electrode through formation of a sulfide bond between unique cysteines, induced by mutation, secured stability, orientation, function, and an efficient electronic junction. The dry-membrane protein in the monolayer retains its capacity to generate a photopotential of approximately +1 V. The photodiode properties, the nanometer-scale dimensions, the high quantum yield, and the almost 60 % energy conversion efficiency make reaction centers intriguing nanotechnological devices for applications in molecular electronics and biotechnology.

Experimental

Site-Directed Mutagenesis: Site-directed mutagenesis in the psaB gene from *Synechocystis sp.* PCC 6803 by homologous recombination using plasmids pZBL, pBLΔB has been previously described [12] (see Supporting Information).

Isolation and Characterization of PS I Complexes: Thylakoid membranes were isolated from isolated cells, and PS I was solublilized by the detergent *n*-dodecyl β-D-maltoside and purified on DEAE-cellulose columns and on a sucrose gradient. The isolation of PS I, the analysis of subunit composition, and the determination of protein and chlorophyll contents and photochemical activity were carried out by

flash-induced transient oxidation of P700 at $\Delta A = 820$ and $\Delta A 700$ nm, as described [11]. Surface-exposed cysteines on PS I were probed by biotin-maleimide, which specifically reacts with the sulfhydryl groups. Biotin-labeled PS I complexes were dissociated and separated by sodium dodecyl sulfate polyacrylamide gel electrophoresis. For immunoblot detection, protein samples were transferred from the gel to nitrocellulose and reacted with peroxidase-conjugated avidin, then developed with enhanced chemiluminescence reagents as previously described [13].

Atomic Force Microscopy: All measurements were made with a commercial atomic force microscope (Nanoscope IIIa MultiMode with Extender Electronics Module, Veeco Instruments, USA). The topography measurements were conducted in tapping mode at a cantilever resonance frequency of 300 kHz.

Kelvin Probe Force Microscopy: The KPFM setup was based on a commercial atomic force microscope (modified NanoScope IIIa MultiMode, Veeco, USA), operating in tapping mode. The electrostatic force is measured in the so-called "lift mode" in this mode, after the topography is measured, the tip is retracted from the sample surface to a fixed height. The oscillation of the tip induced by the piezoelectric device is stopped, and an alternating-current (AC) bias is applied to the cantilever at the same frequency previously used for the topography measurements in the tapping mode. The CPD is extracted in the conventional way by nullifying the output signal of a lock-in amplifier, which measures the electrostatic force at the first resonance frequency [14]. AFM topography and the corresponding KPFM electric potential were recorded in sequential scans at a scan rate of 1 Hz; 512 lines were scanned in two segments over the sample area to form a two-dimensional image. A helium–neon laser ($\lambda = 632.8$ nm, 5 mW cm^{-2}) was switched on for the first segment of the scan and switched off for the second segment.

[1] K. Brettel, *Biochim. Biophys. Acta* **1997**, *1318*, 322.

[2] P. R. Chitnis, N. Nelson, in *Photosynthetic Apparatus: Molecular Biology and Operation*, Vol. 7B (Eds.: L. Bogoras, I. K. Vsil), Academic Press, New York **1991**, p. 177.

[3] J. H. Golbeck, D. A. Bryant, in *Current Topics in Bioenergetics*, Vol. 16 (Ed.: C. P. Lee), Academic Press, New York **1991**, p. 83.

[4] P. Jordan, P. Fromme, H. T. Witt, O. Klukas, W. Saenger, N. Krauss, *Nature* **2001**, *411*, 909.

[5] A. Ben Shem, F. Frolow, N. Nelson, *Nature* **2003**, *426*, 630.

[6] I. Lee, A. Stubna, E. Greenbaum, *J. Phys. Chem. B: Condens. Matter* **2000**, *104*, 2439.

[7] R. Das, P. J. Kiley, M. Segal, J. Norville, A. A. Yu, L. Y. Wang, S. A. Trammell, L. E. Reddick, R. Kumar, F. Stellacci, N. Lebedev, J. Schnur, B. D. Bruce, S. G. Zhang, M. Baldo, *Nano Lett.* **2004**, *4*, 1079.

[8] C. Nakamura, M. Hasegawa, Y. Yasuda, J. Miyake, *Appl. Biochem. Biotechnol.* **2000**, *84*, 408.

[9] S. A. Trammell, L. Y. Wang, J. M. Zullo, R. Shashidhar, N. Lebedev, *Biosens. Bioelectron.* **2004**, *19*, 1649.

[10] Y. Rosenwaks, R. Shikler, T. Glatzel, S. Sadewasser, *Phys. Rev. B* **2004**, *70*, 085 320.

[11] X. M. Gong, R. Agalarov, K. Brettel, C. Carmeli, *J. Biol. Chem.* **2003**, *278*, 19 141.

[12] M. T. Zeng, X. M. Gong, M. C. Evans, N. Nelson, C. Carmeli, *Biochim. Biophys. Acta* **2002**, *1556*, 254.

[13] J. Sun, A. Ke, P. Jin, V. P. Chitnis, P. R. Chitnis, *Photosynthesis: Molecular Biology of Energy Capture* (Ed: Lee McIntosh), Methods in Enzymology, Vol. 297, Academic Press, New York **1998**, p. 124.

[14] O. Vatel, M. Tanimoto, *J. Appl. Phys.* **1995**, *77*, 2358.